Rayleigh scattering of polarized photons

1968 J. Phys. A: Gen. Phys. 1 228

(http://iopscience.iop.org/0022-3689/1/2/307)

J. PHYS. A (PROC. PHYS. SOC.), 1968, SER. 2, VOL. 1. PRINTED IN GREAT BRITAIN

Rayleigh scattering of polarized photons

D. R. S. SOMAYAJULU† and V. LAKSHMINARAYANA
Laboratories for Nuclear Research, Andhra University, Waltair, India
MS. received 8*th August* 1967, *in revised form* 16*th October* 1967

Abstract. Partially polarized photons of energies 0·56 mc^2 and 0·78 mc^2 are produced by Compton scattering in aluminium of gamma rays from a 10·8 Ci ^{137}Cs source. They are used to study the Rayleigh scattering cross sections in two orthogonal planes and the asymmetry ratios are determined at Rayleigh scattering angles 45°, 60°, 75°, 90° and 105° in each case. The data in the two planes are simultaneously collected by using two scintillation counters. The theoretical values of the asymmetry ratios are estimated and compared with the experimental results. In all cases the experimental results are found to be in satisfactory agreement with the theory of Brown and Mayers.

1. Introduction

Four types of elastic scattering processes contribute to the total elastic scattering of gamma rays. Of these processes, Delbruck scattering is not expected to be of any significance for gamma energies less than 1 MeV. Nuclear resonance scattering is important only in a narrow energy region and special arrangements have to be made to compensate for the recoil energy loss in order to observe the process. The contribution of Thomson scattering is small and the cross section for the process shows little angular variation. Thus, for gamma energies less than 1 MeV, Rayleigh scattering is the only process which gives a significant contribution to the elastic scattering cross section. In recent years a number of investigations have been made to detect and study the Delbruck scattering process. The method of study involves the determination of the total elastic scattering cross section and subtraction of the theoretically estimated contributions of all other types of the elastic scattering processes. This subtraction technique yields useful information only if the subtracted contributions are accurately estimated. The contribution of the Rayleigh scattering cross section being the largest, it is essential to estimate this cross section accurately. The earliest theory of Rayleigh scattering is due to Franz (1935) and is based on the form-factor formalism. Brown and Mayers (1954, 1955, 1957) developed a theory for this process, which is more accurate inasmuch as the approximations characteristic of the form-factor formalism are removed. Several experiments have been carried out to determine the elastic scattering cross sections with a view to verifying these theories and also to detecting the Delbruck scattering. While most of these studies were inconclusive in so far as the detection of the Delbruck scattering was concerned, several of them were in agreement with the predictions of Brown and Mayers for the Rayleigh scattering cross sections. The present status of the results of these studies is summarized by Standing and Jovanovich (1962) and Narasimha Murty (1963).

These theories predict the polarization effects in Rayleigh scattering in addition to predicting the cross sections. The studies of the polarization effects are more sensitive tests of the theories. In recent years a few experimental investigations have been made to verify the polarization effects in Rayleigh scattering by Fuschini *et al.* (1960), Manuzio and Vitale (1961), Singh *et al.* (1965) and Williams and McNeil (1965), in which the degree of polarization of the elastically scattered photons was determined for different angles of scattering. Their results were in agreement with the predictions of the theory of Brown and Mayers.

An alternative approach to studying the polarization effects is to determine the Rayleigh scattering cross sections of polarized photons. Brini *et al.* (1958, 1959) adopted this approach and determined the asymmetry ratios R for elastic scattering in two mutually perpendicular planes, employing polarized photons produced by Compton scattering. They used a ^{60}Co

† Now at Physics Department, Indian Institute of Technology, Kanpur, U.P., India.

source of strength 2 Ci, and produced polarized photon beams of energies $0{\cdot}64\,mc^2$ and $1{\cdot}28\,mc^2$. Their results were in agreement with the theory of Brown and Mayers. The present investigation is an extension of their studies with the following improvements:

(i) A monoenergetic ^{137}Cs source of strength 10·8 Ci is used in preference to a ^{60}Co source (strength 2 Ci).

(ii) An aluminium scatterer is used in preference to copper to produce the polarized photon beams inasmuch as the bound-electron scattering effects are considerably reduced.

(iii) Two well-matched detectors are used in the two planes to collect simultaneously the scattered events instead of successively collecting the data by rotating the same detector as in the case of the earlier study.

The asymmetry ratios are determined at Rayleigh scattering angles 45°, 60°, 75°, 90° and 105° in lead for incident photon energies $0{\cdot}56\,mc^2$ (degree of polarization 0·58) and $0{\cdot}78\,mc^2$ (degree of polarization 0·50), and compared with the theoretical predictions of Franz and Brown and Mayers.

2. Experimental details

The experimental arrangement is shown in figure 1. The ^{137}Cs source of strength 10·8 Ci is housed in a source holder 2 ft diam. × 2 ft high made of lead. The source holder has a 1 in. central brass tube, into which the source could be introduced and fixed

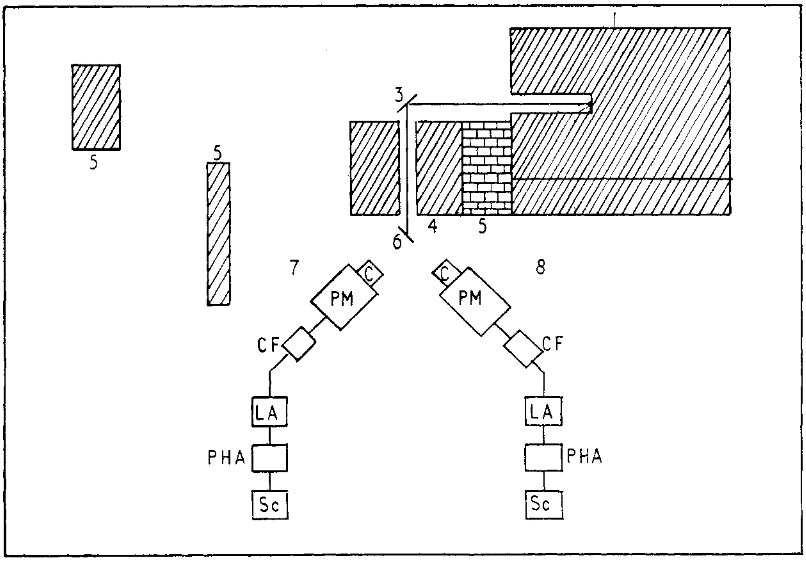

Figure 1. A schematic arrangement of the experimental set-up: 1, source holder; 2, source (10·8 Ci ^{137}Cs); 3, aluminium scatterer; 4, collimator for the scattered photon beam; 5, additional lead shielding; 6, lead scatterer; 7, scintillation counter in the horizontal plane; 8, scintillation counter in the orthogonal plane; C, crystal (NaI(Tl)); PM, photomultiplier; CF, cathode follower; LA, linear amplifier (non-overloading type); PHA, pulse-height analyser; Sc, scaler.

at any position. A lead-filled brass tube with a conical opening is used to collimate the gamma rays, the diameters of the hole on the source and target sides being $\frac{1}{4}$ in. and $\frac{3}{4}$ in., respectively. The target is an aluminium cylinder of dimensions $\frac{1}{2}$ in. diam. × $\frac{3}{4}$ in. high. The Compton-scattered partially polarized photon beam is further collimated by means of a lead block 8 in. high × 8 in. wide × 4 in. thick, containing an exit hole of 1 in. diam. The collimated beam traverses a lead scatterer in the form of a hollow cylinder of 0·39 in. diam. × 0·39 in. high, the wall thickness being 0·039 in. This form is selected for the scatterer to minimize the self-absorption and also to provide a symmetrical geometry for counting in the two planes. The elastically scattered photons from this lead target are detected in two NaI(Tl) crystals ($1\frac{1}{2}$ in. diam. × 1 in. high) attached to DuMont 6292 photomultipliers. The pulses, after amplification and pulse-height analysis, are applied to decade scalers. One of the two scintillation counters is placed in the horizontal plane and could be rotated about the target centre to detect the elastic scattering events at different angles in this plane. The other scintillation counter is arranged in the orthogonal plane and could be rotated in a suitable way along with the one in the horizontal plane so as to place it orthogonally for each angular position. The following auxiliary experiments are conducted:

(*a*) Initially a well-matched pair of photomultipliers and NaI(Tl) crystals are selected. Finally, the photopeak efficiencies, resolutions and energy linearities of the two scintillation counters are studied using monochromatic sources ^{170}Tm, ^{141}Ce, ^{203}Hg and ^{137}Cs. The high-tension voltages and amplifications are slightly adjusted to yield nearly identical performances of the two counters in the chosen energy region (84 kev to 662 kev).

(*b*) The diffuse background in the detectors is recorded for various detector positions (with the two targets removed), and it is minimized by the use of suitable additional lead shielding.

(*c*) The spectra are recorded for various aluminium target sizes to select the optimum size as a compromise between the angular spreads (and the consequent depolarization effects) and large intensities.

(*d*) The spectra are recorded for different lead target sizes to select the optimum size to maximize the elastic events detected.

(*e*) The intrinsic asymmetry of the set-up is initially studied by replacing the lead target by a source of monochromatic gamma rays (^{203}Hg, 279 kev) spread over dimensions equivalent to the lead target. The count rates in the high-energy halves of the respective photopeaks are assumed to indicate the intrinsic asymmetry. Since the two scintillation counters are adjusted (see (*a*) above) for nearly identical performance, the geometrical positions of the counters are slightly adjusted to yield the intrinsic asymmetry less than 0·5%. The intrinsic asymmetries in other angular positions are likewise studied to ensure that the initial adjustment is accurate and does not introduce any systematic errors.

The spectrum of scattered photons for a Rayleigh scattering angle of 90° recorded in the scintillation counter placed in the scattering plane is shown in figure 2. In this case the

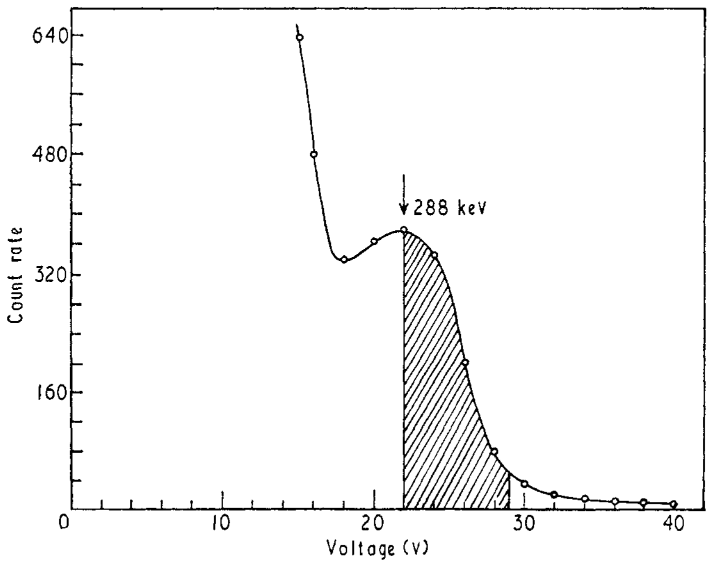

Figure 2. Spectrum of the Rayleigh-scattered photons at 90° in lead for incident partially polarized photons ($h\nu = 0{\cdot}56\,mc^2$, $\xi = 0{\cdot}58$) recorded in the scintillation counter placed in the horizontal plane. The abscissa represents the base-line voltage of the pulse-height analyser used to record the spectrum. The shaded area represents the events selected in the window of the pulse-height analyser in the final counting.

partially polarized photons are of energy 288 kev (corresponding to the Compton scattering angle of 90°), the degree of polarization (defined in the notation of Brini *et al.*) being 0·58. It can be seen from the figure that a broad peak appears at 288 kev, the low-energy side of which increases steeply. In general, the scintillation counter receives four types of events, in addition to background and scattered events from the target holder:

1. Elastic–elastic events: these correspond to the primary photons elastically scattered by aluminium and subsequently elastically scattered by lead.
2. Elastic–inelastic events: photons elastically scattered by aluminium and subsequently inelastically scattered by lead.
3. Inelastic–elastic events: primary photons inelastically scattered by aluminium and subsequently elastically scattered by lead.
4. Inelastic–inelastic events: primary photons inelastically scattered by aluminium and subsequently inelastically scattered by lead.

In order to obtain an orientation of the relative number of these different types of events, the respective cross sections have been employed and the relative intensities of the four types of events are obtained. These values, normalized to the inelastic–elastic events (type 3 events—the desired type) for the 90° scattering case are given in table 1.

Table 1. Relative intensities of the different types of events

Ser. No.	Type of events	Peak position (kev)	Relative intensity
1	elastic–elastic	662	$6{\cdot}9 \times 10^{-10}$
2	elastic–inelastic	288	$2{\cdot}9 \times 10^{-7}$
3	inelastic–elastic	288	1·0
4	inelastic–inelastic	184	31·8

It can be seen from the table that the relative magnitudes are in increasing order from type 1 to type 4 events. The type 1 events contribute to the high-energy side of the desired peak. The type 2 and type 3 events, being of the same energy, occur in the 288 kev peak. However, it can be seen from table 1 that the contribution of type 2 events is quite negligible. The low-energy side of the 288 kev peak receives a contribution from the type 4 events, and is represented by the steeply increasing part in figure 2. In order to select the desired events and discard the undesired ones, the channel in the pulse-height analyser of the scintillation spectrometer is set to accept the high-energy half of the 288 kev peak (shaded area in figure 2).

The accepted channel also includes some undesired events due to background and the scattering from the target holder. Hence an auxiliary experiment is conducted to assess these contributions with the target removed from the target holder. The difference between the number of events in the accepted channel with and without the target on the target holder represents the number of elastic events. The scintillation counter in the orthogonal plane is likewise adjusted to accept the high-energy half of the desired peak.

The actual experiment consisted in collecting the count rates in the accepted channels and obtaining the asymmetry ratio R (defined as the ratio of the elastic events recorded in the counter placed in the horizontal plane to those in the orthogonal plane). A minimum of 10 000 elastic events are collected in the scintillation counter placed in the orthogonal plane. The corresponding number in the horizontal plane is always higher. The contributions of background and the target holder are determined by collecting counts for equal times with no target in the polarized photon beam. The background slightly varied for the different angles and consequently resulted in different values for the signal-to-noise ratio. In the most favourable case, corresponding to the Rayleigh scattering angles of 45°, the signal-to-noise ratio is about 8 and decreased to about 1 for the scattering angle of 90°. In order to conduct the experiment at a Rayleigh scattering angle of 105°, the target holder had to be moved further away from the collimator. Owing to the decreased intensities of the partially polarized photons, as well as the decrease in the Rayleigh scattering cross section, it was not possible to collect more than about 4000 elastic events in a reasonable experimental time. Under these conditions the signal-to-noise ratio dropped to about 0·03.

Although the true counts collected at the different angles remained about the same (except at 105°), the actual error in the determination of the asymmetry ratio R is determined by the signal-to-noise ratio. In addition to the signal-to-noise ratio, the effect of inadequate separation of the events of type 3 and type 4 is also considered. In the case of scattering corresponding to 90° (see figure 2), setting the channel width to accept the events in the high-energy half of the spectrum, to a great extent, removed type 4 events. But at smaller angles of scattering, the relative energy separations between the events corresponding to types 3 and 4 being smaller, the separation is more difficult. In the cases of angles of scattering 60° and 45° there is thus an additional source of error even after shifting the position of the accepted channel towards higher energies. Taking into account this contribution, together with the signal-to-noise ratio and the collected counts, the errors are estimated and found to vary from 1·5% at 45° to 3·5% at 90°. At the Rayleigh scattering angle of 105°, however, owing to the reduced count rates as well as the signal-to-noise ratio, the error has increased to about 10%.

3. Theoretical computations

The degree of polarization of a partially polarized photon beam produced in the Compton scattering (in the notation of Brini *et al.*) is given by

$$\xi = \frac{-\sin^2\theta_C}{1+\cos^2\theta_C+(K_0-K)(1-\cos\theta_C)} \tag{1}$$

where θ_C is the Compton scattering angle and K_0 and K are the incident and scattered photon energies in mc^2 units.

The Rayleigh scattering cross section, according to the theory of Franz, at an angle θ for an incident partially polarized photon beam is given by

$$\frac{d\sigma}{d\Omega} = r_0{}^2F^2\{(1+\cos^2\theta)+\xi(\cos^2\theta-1)\} \tag{2}$$

where r_0 is the classical electron radius and F is the form factor. The corresponding expression, according to the theory of Brown *et al.*, is given by

$$\frac{d\sigma}{d\Omega} = r_0{}^2\{(AA^*+BB^*)+\xi(AB^*+A^*B)\} \tag{3}$$

where

$$A = M(1',1)+M(2',2)$$

and

$$B = M(1',2)+M(2',1).$$

The functions M occurring in the above relations are the transition amplitudes between the left spinning circular polarization states of the incident (1 and 2) and the scattered (1′ and 2′) photons.

The asymmetry ratio R for elastic scattering in the horizontal and the orthogonal planes in the notation of Brini *et al.* is given by

$$R = \frac{d\sigma_0/d\Omega+\xi(d\sigma_1/d\Omega)}{d\sigma_0/d\Omega-\xi(d\sigma_1/d\Omega)} \tag{4}$$

where $d\sigma_0/d\Omega$ and $d\sigma_1/d\Omega$ are the elastic scattering cross sections for polarization-independent and polarization-dependent parts, respectively. The values of R are estimated from equations (2), (3) and (4).

The variation of R with Rayleigh scattering angle θ is shown in figures 3 and 4 for $0{\cdot}56\ mc^2$ and $0{\cdot}78\ mc^2$, corresponding to $\theta_C = 90°$ and $60°$ respectively.

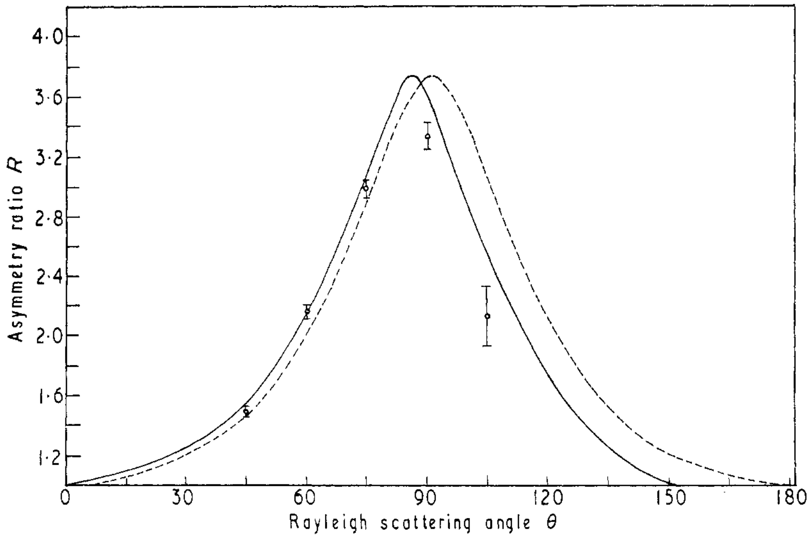

Figure 3. Plot of the asymmetry ratio R as a function of the Rayleigh scattering angle, for polarized photons (ξ = 0·58) of energy 0·56 mc^2. The full and broken curves represent the results of the theory of Brown *et al.* and Franz, respectively. The experimental values of R are also shown in the figure.

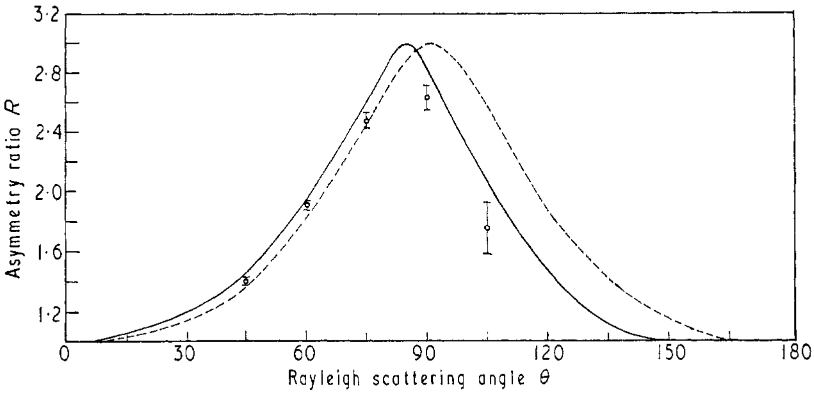

Figure 4. Plot of the asymmetry ratio R as a function of the Rayleigh scattering angle for polarized photons (ξ = 0·50) of energy 0·78 mc^2. The full and broken curves represent the theoretical values of Brown *et al.* and Franz, respectively. The experimental values of R are also shown in the figure.

4. Results and discussions

The values of asymmetry ratios R are determined for partially polarized photons produced by Compton scattering at 90° ($h\nu$ = 0·56 mc^2, ξ = 0·58) and 60° ($h\nu$ = 0·78 mc^2, ξ = 0·50) at Rayleigh scattering angles of 45°, 60°, 75°, 90° and 105° in each case. The entire equipment is housed in an air-conditioned room with adequate air circulation. The counts in the accepted channels are collected at regular intervals to check the reproducibility and ensure negligible channel drifts. Several sets are collected, and the best of them, which are adjudged to show no channel drifts, are accepted. The values, obtained as a mean of four such values in each case, are given in tables 2 and 3 together with the corresponding theoretical values.

The theoretical values are not corrected for angular spreads involved in the experiment. The first scatterer being small (Al cylinder of $\frac{1}{2}$ in. diam. × $\frac{3}{4}$ in. high), the angular spread of the collimated beam traversing the second scatterer (hollow lead cylinder of

Table 2. Values of asymmetry ratios, $h\nu = 0{\cdot}56\ mc^2$, $\xi = 0{\cdot}58$

Ser. No.	Rayleigh scattering angle θ	Experimental values of R	Theoretical values of R: Theory of Franz	Theory of Brown *et al.*
1	45°	$1{\cdot}50 \pm 0{\cdot}02$	1·48	1·56
2	60°	$2{\cdot}17 \pm 0{\cdot}04$	2·06	2·20
3	75°	$2{\cdot}99 \pm 0{\cdot}07$	2·94	3·16
4	90°	$3{\cdot}36 \pm 0{\cdot}11$	3·75	3·55
5	105°	$2{\cdot}15 \pm 0{\cdot}21$	3·00	2·44

Table 3. Values of asymmetry ratios, $h\nu = 0{\cdot}78\ mc^2$, $\xi = 0{\cdot}50$

Ser. No.	Rayleigh scattering angle θ	Experimental values of R	Theoretical values of R: Theory of Franz	Theory of Brown *et al.*
1	45°	$1{\cdot}41 \pm 0{\cdot}02$	1·40	1·46
2	60°	$1{\cdot}91 \pm 0{\cdot}03$	1·85	1·99
3	75°	$2{\cdot}48 \pm 0{\cdot}06$	2·50	2·60
4	90°	$2{\cdot}63 \pm 0{\cdot}09$	2·99	2·79
5	105°	$1{\cdot}76 \pm 0{\cdot}18$	2·55	2·00

0·39 in. diam. × 0·39 in. high × 0·039 in. thick) is small (of the order of 4°) and is not expected to produce considerable depolarization effects. However, the angular spreads involved in the second scattering are not negligible inasmuch as the detectors are NaI(Tl) crystals of $1\frac{1}{2}$ in. diam. × 1 in. high and placed at small distances from the scatterer for reasons of intensity. The actual angular spreads involved slightly varied in the range of scattering angles investigated. For the case of scattering at 90°, $\Delta\theta = 48°$ and $\Delta\phi = 42°$. These are evaluated in an approximate way, the finite size of the lead scatterer being taken into account. Thus the theoretical values have to be corrected for this effect before comparing them with the experimental values; but it is not possible to do so inasmuch as the explicit ϕ dependence of the Rayleigh scattering cross section is not available. However, as an approximate measure, we studied the depolarization effects, taking into account the θ dependence of the Rayleigh scattering cross section and carrying out the numerical integrations over $\Delta\theta$. It is concluded from such an analysis that (although the individual values of the numerically integrated cross sections did show 6 to 10% variations) the values of the asymmetry ratios are only attenuated by about 2%. The theoretical values are therefore likely to be smaller than the values included in the tables by about 2%.

Allowing for the depolarization effects outlined above, it is reasonable to conclude that the present experimental values support the theoretical values of Brown *et al.* Apart from the magnitudes of the asymmetry ratios, a comparison on the basis of the trend of variation of the asymmetry ratio with the Rayleigh scattering angle (see figures 3 and 4) yields the result that the experimental values of the asymmetry ratio definitely support the theory of Brown *et al.* It can be seen from figures 3 and 4 that, although the experimental values of R at 45°, 60° and 75° fall between the two theoretical curves, they will show better agreement with the theoretical values after the depolarization effects mentioned above have been allowed for.

In the case of $0{\cdot}78\ mc^2$ the intensity of the partially polarized photons is larger owing to the increased Compton scattering cross section. The background also increased slightly and the signal-to-noise ratios are maintained at about the same values as in the case of $0{\cdot}56\ mc^2$ by employing additional shielding.

As the 'free-electron hypothesis' is quite valid in the case of Compton scattering in aluminium, the scattering from bound electrons is not expected to play a significant role in this investigation. It is found in the computations that the contribution of the Thomson scattering cross section forms about 0·5% (or less) of the Rayleigh scattering cross section in all cases of interest in the present study. Hence the contribution from the Thomson scattering could be neglected.

The present investigation therefore leads to the conclusion that the theory of Brown and Mayers is well founded and could be used to predict accurately the Rayleigh scattering cross sections as well as their polarization effects.

References

BRINI, D., FUSCHINI, E., MURTY, D. S. R., and VERONESI, P., 1959, *Nuovo Cim.*, **11**, 533–45.
BRINI, D., FUSCHINI, E., PELI, L., and VERONESI, P., 1958, *Nuovo Cim.*, **8**, 877–90.
BROWN, G. E., and MAYERS, D. F., 1954, *Proc. R. Soc.* A, **227**, 51–8, 59–72.
—— 1955, *Proc. R. Soc.* A, **234**, 387–90.
—— 1957, *Proc. R. Soc.* A, **242**, 89–95.
FRANZ, W., 1935, *Z. Phys.*, **95**, 652–68.
—— 1936, *Z. Phys.*, **98**, 314–20.
FUSCHINI, E., MURTY, D. S. R., and VERONESI, P., 1960, *Nuovo Cim.*, **15**, 847–9.
MANUZIO, G., and VITALE, S., 1961, *Nuovo Cim.*, **20**, 638–47.
NARASIMHA MURTY, V. A., 1963, *D.Sc. Thesis*, Andhra University.
SINGH, M., ANAND, S., and SOOD, B. S., 1965, *Nuovo Cim.*, **35**, 1047–51.
STANDING, K. G., and JOVANOVICH, J. V., 1962, *Can. J. Phys.*, **40**, 622–53.
WILLIAMS, R. A., and MCNEIL, K. G., 1965, *Can. J. Phys.*, **43**, 1078–87.